JOURNAL OF VIROLOGY, Mar. 1995, p. 1389–1399
0022-538X/95/$04.00+0

Vol. 69, No. 3

Quantification of Transcripts from the ICP4 and Thymidine Kinase Genes in Mouse Ganglia Latently Infected with Herpes Simplex Virus

MARTHA F. KRAMER AND DONALD M. COEN*

Department of Biological Chemistry and Molecular Pharmacology and Committee on Virology, Harvard Medical School, Boston, Massachusetts 02115

Received 6 October 1994/Accepted 17 November 1994

Herpes simplex virus establishes latency in nervous tissue in which it is maintained for the life of the mammalian host, with occasional reactivation leading to subsequent spread. Latency-associated transcripts are abundant during latency, but viral proteins and productive cycle RNAs have not been detected. Using sensitive, quantitative PCR assays, we have quantified certain viral RNAs specific to productive-cycle genes in mouse ganglia latently infected with herpes simplex virus type 1. Sense-strand RNA specific to the essential immediate-early gene, *ICP4*, was present in most ganglia in variable amounts relative to the amount of viral DNA, with one to seven molecules of RNA per viral genome in about 20% of ganglia. In contrast, the amount of latency-associated transcripts was much less variable, at an average of 4×10^4 molecules per viral genome. The amounts of *ICP4*-specific RNA were similar at 30 and 60 days postinfection, and at least some of these transcripts initiated within a region consistent with utilization of the *ICP4* promoter. RNA specific to the thymidine kinase gene, whose transcription in productive infection is dependent on ICP4, was present in latently infected ganglia at a maximum level of 3.2×10^6 molecules per ganglion (500 molecules per viral genome). *ICP4*-specific and *tk*-specific RNAs measured from the same samples showed a positive correlation extending over 2 orders of magnitude. We conclude that *ICP4*-specific RNA is expressed in the absence of detectable reactivation and discuss possible implications of our findings for latent gene expression.

Herpes simplex virus (HSV) can express two distinct transcriptional patterns, one specifying productive infection and the other specifying latency. Productive infection, which is typical at peripheral sites in the mammalian host and in cultured cells, involves a regulated cascade of gene expression. Immediate-early (IE) genes are expressed first and are required for the efficient expression of the subsequent early (E) and late (L) genes. The productive cascade generates the components required for viral replication and generation of infectious progeny. In contrast, latency is characterized by a complete lack of detectable infectious virus. The only viral products that are abundantly expressed are the latency-associated transcripts (LATs) (11, 14, 60, 66, 70), which are not abundant during productive infection. No infectious virus or viral antigens have been detected in homogenized human autopsied trigeminal ganglia (3) or mouse trigeminal or dorsal root ganglia latently infected with HSV type 1 (HSV-1) (9, 15, 19, 35, 41, 44, 49, 52, 63, 65, 66, 67, 69), although reactivation competence can be demonstrated by explant of tissue and other methods. The absence of infectious virus and detectable viral antigens correlates with the absence of detection of transcripts from productive-cycle genes in human trigeminal or sacral ganglia infected with HSV-1 (11, 12, 23, 68) or HSV-2 (10) or mouse trigeminal or dorsal root ganglia latently infected with HSV-1 (14, 15, 19, 20, 55, 56, 66, 70, 76) or HSV-2 (71, 73). However, infectious virus and viral products can be readily detected during the acute phase of establishment of latency and during reactivation. The mechanisms by which the productive pattern of gene expression in acutely infected neurons switches to the latent pattern, and how productive transcription is reactivated, remain central unanswered questions in HSV biology, with significance for the areas of tissue-specific gene expression and control of HSV disease.

Part of the difficulty in studying gene expression in latency is the low proportion of latently infected cells in the target tissue and the resultant difficulties in detecting rare RNAs. The advent of PCR technology has enabled the quantitative detection of nucleic acids at the level of individual molecules (61). To ascertain whether there is a low level of HSV gene expression other than LATs during latency, we have developed a sensitive quantitative RNA PCR (QRPCR) assay for HSV genes. We have applied this assay to detect HSV RNAs in latently infected mouse trigeminal ganglia, in particular to the IE gene *ICP4* because of its critical role in activation of E and L genes (16, 53). It has been thought that the absence of IE expression in latency permits establishment and maintenance of latency, and activation of IE genes would lead to reactivation (34, 45, 48, 63, 70, 78). We report the measurement and quantification of *ICP4*-specific RNA at the level of hundreds to tens of thousands of molecules per ganglion, or from 0.004 to 7 *ICP4* RNA molecules per viral genome copy, and compare its expression with that of LATs and thymidine kinase gene (*tk*)-specific RNA. We discuss the results of this study in terms of models of mechanisms of latency and reactivation.

MATERIALS AND METHODS

Viruses and cells. The KOS strain of HSV-1 was propagated and assayed on Vero cell monolayers as previously described (7). The *tk* deletion mutant *dl*sptk has been previously described (8). The LAT promoter deletion mutant *dl*LAT1.8 has been previously described (43) and was generously provided by P. Schaffer.

Infection of mice and tissue collection. Eight-week-old CD-1 outbred mice were inoculated with 2×10^6 PFU of virus or mock infected with virus diluent via corneal scarification (44). At 30 or 60 days postinoculation (p.i.), trigeminal ganglia were removed and rapidly frozen in liquid nitrogen. The elapsed times

* Corresponding author. Mailing address: Department of Biological Chemistry and Molecular Pharmacology, Harvard Medical School, 250 Longwood Ave., Boston, MA 02115. Phone: (617) 432-1691. Fax: (617) 432-3833. Electronic mail address: dcoen@warren.med.harvard.edu.

TABLE 1. Primers and probes

Gene	Oligonucleotide[a]	Sequence (5′ to 3′)	Product size (nt)
Mouse adipsin[b]	MT-1	AGT GTG CGG GGA TGC AGT	48
	MT-2	ACG CGA GAG CCC CAC GTA	
	MT-3	AGT CGA AGG TGT GGT TAC	
Mouse β-actin	Act-1	AAC CCT AAG GCC AAC CGT GAA AAG ATG ACC	379
	Act-2	CCA GGG AGG AAG AGG ATG CGGC	
	Act-3	GCT CTA GAC TTC GAG CAG GAG ATG GCC ACT	
LAT	L-1	GAC AGC AAA AAT CCC CTG AG	195
	L-2	ACG AGG GAA AAC AAT AAG GG	
	L-3	CGA CAC GGA TTG GCT GGT GT	
ICP4	4-1	CGA CAC GGA TCC ACG ACC C	101
	4-2	GAT CCC CCT CCC GCG CTT CGT CCG	
	4-3	ACC GCC AGA GAC AGA CCG TCA GA	
tk[b]	tk-1	CTT AAC AGC GTC AAC AGC GTG CCG	60
	tk-2	CAA AGA GGT GCG GGA GT	
	tk-3	CAG ATC TTG GTG GCG TG	

[a] Numbering indictes the following: 1, upstream primer; 2, downstream primer; 3, internal probe.
[b] Sequences were as reported by Katz et al. (33).

from cervical dislocation to immersion of tissue in liquid nitrogen were 137 ± 21 (mean ± standard deviation [SD]) s for left ganglia and 195 ± 23 s for right ganglia (n = 18 each).

Preparation of ganglionic DNA and RNA. Ganglionic nucleic acids were prepared by the method of Chirgwin et al. (5), with attention to optimizing recovery and maintaining PCR-contaminant-free reagents and conditions. Briefly, each ganglion was transferred from liquid nitrogen to 1.0 ml of guanidine thiocyanate (GTC) solution (5 M GTC, 50 mM Tris [pH 7.5], 10 mM EDTA, 5% β-mercaptoethanol) and homogenized in an acid-washed, autoclaved Kontes size 20 glass tissue grinder. To analyze DNA, a 100-μl aliquot was transferred to a screw-cap tube and mixed with 300 μl of water, 40 μl of 3 M sodium acetate, and 1.0 ml of absolute ethanol. After incubation at −20°C for at least 1 day, the precipitate was collected by centrifugation at 16,000 × g for 30 min, washed with 70% ethanol, and resuspended in water (sterile water for irrigation; Baxter). In early experiments, the pellet was resuspended in 50 μl of water, extracted and back-extracted with phenol-chloroform (1:1), extracted with chloroform, and ethanol precipitated by using 0.5 volume of 7.5 M ammonium acetate, after which PCR analyses of cellular and viral DNA were performed with aliquots of the resuspended pellet. Because of low and variable yield, the method was changed to the following. The resuspended pellet was brought to a final volume of 50 μl containing 0.2 μg of proteinase K per ml, 0.02% Tween 20, 1× PCR buffer (50 mM KCl, 10 mM Tris-HCl, pH 9.0 [at 25°C], 0.1% Triton X-100), and 1.5 mM $MgCl_2$ and heated sequentially to 65°C for 2 h, 80°C for 20 min, and 94°C for 10 min to inactivate the enzyme. Aliquots were taken directly for PCR analysis. DNA standards were prepared from HSV DNA quantified by comparison with standards as described previously (33), reconstituted with uninfected mouse ganglia, and processed as described for the tissue samples. To analyze RNA, sarcosyl (*N*-lauroylsarcosine; Sigma) was added to the remaining 900 μl of GTC homogenates to 0.5%, and the homogenates and two 0.8-ml GTC washes of the tissue grinder and transfer syringe were layered onto 2.0-ml 5.7 M cesium chloride cushions. Total RNA recovered after equilibrium centrifugation and ethanol precipitation (5) was treated with 15 U of RNase-free DNase (Promega) in the presence of 1 U of RNasin (Promega) per 40 μl of reaction mixture for 1 h at 37°C. The reaction was stopped with the addition of EDTA to 0.5 M and 1 μg of yeast tRNA (Boehringer Mannheim) and then extracted with phenol-chloroform (1:1), back-extracted with water, extracted with chloroform, and ethanol precipitated by using ammonium acetate.

Reverse transcription. Following an initial denaturation step of 10 min at 95°C, total recovered RNA was hybridized with downstream primers Act-2, 4-2, L-2, tk-2 (Table 1), and other HSV-1-specific oligonucleotides (not described in this report) for 4 to 16 h at 65°C in a 12-μl volume containing 3 pmol of each downstream primer, 250 mM KCl, 10 mM Tris (pH 8.3), and 1 mM EDTA and then covered with an oil overlay. After phase inversion with chloroform, half (6 μl) of each sample was added to each of two reaction mixtures containing 12 μl of 1.5× reverse transcriptase (RT) buffer (1.5 mM deoxynucleoside triphosphates [dNTPs], 7.5 mM dithiothreitol, 15 mM $MgCl_2$, 0.09 M KCl, 0.63 mM Tris [pH 8.3]) (1). Reaction mixtures were incubated with or without 10 U of avian myeloblastosis virus RT (Promega) at 42.5°C for 1 h and then subjected to heat denaturation at 95°C for 5 min. The resulting cDNA samples were stored at −80°C.

RNA standards. Plasmid pSPMβA, generously provided by S. Sakiyama, contains the mouse β-actin cDNA under the control of the bacterial SP6 promoter (74). HSV genes and plasmids containing relevant fragments are shown in Fig. 1. Plasmid pKS+5′ICP4 was constructed, using standard techniques (2), by cloning the 2.5-kb *Eco*RI-*Bam*HI fragment of pK1-2 (17) (kindly provided by D. Knipe) containing the 5′ end of the *ICP4* gene into the *Eco*RI and *Bam*HI sites of Bluescript II KS+ (Stratagene), placing it under the control of the bacterial T3 promoter and enabling antisense transcription of this region from the T7 promoter (Fig. 1C). Plasmid pSVtk containing the *Eco*RI-*Pvu*II fragment including the *tk* gene was kindly provided by Charles Hwang (28) (Fig. 1D). Plasmid pKS+5′LAT was constructed by cloning the *Eco*RV-*Sal*I 2.3-kb fragment of the LAT 5′ region from pRFS (43) (kindly provided by P. Schaffer) into the *Eco*RV and *Sal*I sites of Bluescript II KS+, placing it under the control of the T3 RNA polymerase (Fig. 1E). RNA transcriptions in vitro were performed by using 2 μg of linearized plasmid DNA in 100-μl reaction volumes as described elsewhere (54), with low-specific-activity incorporation of [^{35}S]GTP (New England Nuclear) (25 μCi in 20 μmol per reaction). After the 2-h reaction, one aliquot of each reaction was separated electrophoretically alongside radiolabeled RNA size markers transcribed concurrently on a formaldehyde-agarose gel (2), which was dried and subjected to autoradiography, to verify that RNA of the predicted size was the only detectable product. Another aliquot was taken to measure total counts per minute for determination of percent incorporation. Following treatment with RNase-free DNase (Promega), phenol-chloroform extraction, and ethanol precipitation, the samples were resuspended in 100 μl of nuclease-free water (Promega). Triplicate aliquots were taken for measurement of trichloroacetic acid-precipitable counts at this point to account for any loss incurred during the extraction procedure. The amount of RNA was calculated from the percentage of incorporated GTP (trichloroacetic acid-precipitable counts divided by total counts) times the amount of GTP present in the reaction mixture (50 nmol), corrected for the G+C content of individual transcripts (50% for β-actin [74], 80% for *ICP4* [47], 65% for LAT [77], and 62% for *tk* [31]), the size in nucleotides of each transcript, and Avogadro's number. These synthetic RNA stocks were stored in aliquots at −80°C. Equivalent amounts of quantified standard RNA (LAT, *tk*, and *ICP4* with other HSV-1-specific sequences not described here) were combined, serially diluted, and reconstituted with 5 μg of total cellular RNA prepared from mouse brain (by the GTC-cesium chloride method [2]) or total RNA from individual uninfected mouse trigeminal ganglia (as described above). β-Actin standard serial dilutions were reconstituted with 5 μg of yeast tRNA (Boehringer Mannheim). For each set of samples, reconstitution standards were made and sample and standard cDNAs were prepared concurrently, as described above, using the same DNase and RT enzyme lots, reagents, and equipment to control for assay-to-assay variability.

PCR. PCR mixtures were brought to a volume of 90 μl containing 10 μl of 10× buffer (500 mM KCl, 100 mM Tris-HCl, pH 9.0 [at 25°C], 1.0% Triton X-100; Promega), 50 pmol of each upstream and downstream primer (Table 1), $MgCl_2$ at a concentration unique to each assay (Table 2), and sample or standard DNA or cDNA. Following heat denaturation at 95°C for 5 min (hot-start method [6]), 10 μl containing 2.5 U of *Taq* polymerase (Promega) and 0.8 μl of 25 mM dNTPs (Promega) (for a final reaction concentration of 200 μM) was added, and the samples were overlaid with mineral oil. Water blanks and positive controls containing 2, 20, 200, and 2,000 molecules of HSV genomic DNA were included with each assay. Amplifications were performed on a Perkin-Elmer Cetus DNA Thermal Cycler with denaturation for 1.0 min at 94°C, annealing for 1.0 min at 55 or 60°C (Table 2), and extension for 1.0 min at 72°C for the total number of cycles listed in Table 2. Reaction mixtures were stored at 4°C. Coamplification of viral (*tk*) and cellular (adipsin) DNA was performed and analyzed as previously described (33) on 10 μl of sample but with the inclusion of the hot-start method, reduction of the *Taq* polymerase to 2.5 U, and shortening of the annealing and extension steps to 1.0 min each. Assays for RNA were performed separately for each gene sequence to be amplified, using a portion of the cDNA (0.5 μl each for

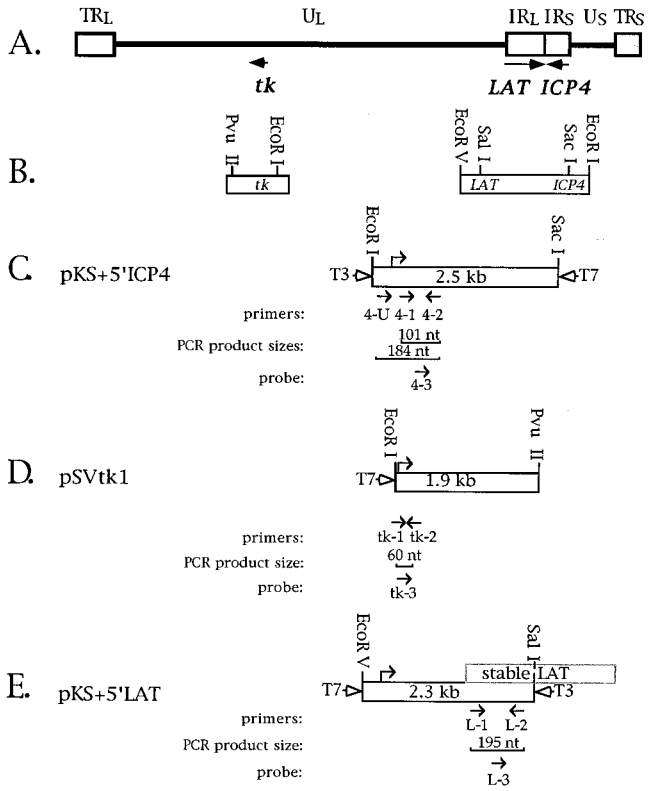

FIG. 1. Regions of the HSV-1 genome assayed. (A) Genome structure. The boxes represent the terminal and internal repeat (TR and IR) regions which bracket the unique long and short (U_L and U_S) sequences depicted in the prototype arrangement. Arrows below the genome diagram designate the map locations and orientations of the *tk*, *ICP4*, and LAT genes. (B) Expanded regions containing genes of interest showing restriction enzyme sites used for cloning into transcription plasmids. (C to E) Open boxes represent the portions of each gene which were cloned into transcription plasmids, with the size of the insert in kilobase pairs indicated in each box. The restriction enzyme sites indicated above each box correspond to those shown in panel B. The transcription start site is indicated as a bent arrow above each box. The identities and directions of bacterial polymerase promoters are indicated at the sides of the boxes for T7 and T3 RNA polymerases. Below each box, arrows indicate the directions and relative positions of PCR primers (numbered 1 and 2) and probes (numbered 3), with the identities indicated underneath each. The size of each PCR product is indicated in number of nucleotides. (C) The *ICP4* transcription plasmid, pKS+5′ICP4, which contains the 5′ half of the *ICP4* gene cloned into the Stratagene Bluescript II KS+ vector. (D) The *tk* transcription plasmid, pSVtk1 (28). (E) The LAT transcription plasmid, pKS+5′LAT, which contains the 2.3-kb *Eco*RV-to-*Sal*I 5′ region cloned from pRFS (43) into Bluescript II KS+. Superimposed on the cloned sequence is a box representing the genomic location of the 2-kb LAT, labeled "stable LAT."

LAT and β-actin and 3.0 μl each for *ICP4* and *tk*). Product sizes are indicated in Fig. 1 and Table 1. Product specificity was verified by predicted size, hybridization with the internal oligonucleotide probe, and restriction endonuclease analysis.

Detection and quantification of PCR products. Reaction products (10 μl) were separated by electrophoresis on a nondenaturing polyacrylamide gel of 8% for β-actin or LAT, 10% for *ICP4*, or 12% for *tk* or adipsin. Gels were stained with ethidium bromide and visualized under UV light. Stained bands which were characteristic for each assay and which did not all coincide with the specific PCR product were observed. These nonspecific products were similar in mock-infected and virus-infected samples, showing that they arose from cellular sequences. Separated products were electroblot transferred to a nylon filter (GeneScreen Plus; NEN), UV cross-linked for 5 min, and prehybridized, probed, and washed as previously described (33). Probes (Table 1) were end labeled with [γ-^{32}P]ATP (ICN) to high specific activity (range, 5×10^8 to 7×10^8 cpm/μg). Filters were exposed to preflashed Kodak XAR-5 film with intensifying screens at −80°C for 16 to 24 h. Filters were additionally exposed to a storage PhosphorImager cassette (Molecular Dynamics) for 2 to 24 h and quantified according to the manufacturer's protocol. Data were analyzed with Microsoft Excel and Cricketgraph software packages and a Macintosh IIvx computer.

TABLE 2. PCR conditions

Gene	[Mg^{2+}] (mM)	Additive	Annealing temp (°C)[a]	No. of cycles[b]
Mouse adipsin	3.0	PMPE[c]	55	30
Mouse β-actin	1.5	PMPE	60	24
LAT	2.5		55	18
ICP4	1.5		60	30
tk	4.5		55	30

[a] In each case, the melting temperature was 94°C and the extension temperature was 72°C. Each temperature was held for 1.0 min.
[b] The cycle number reflects the relative abundance of a given RNA species.
[c] PMPE, Perfect Match Polymerase Enhancer (Stratagene).

Normalization of viral DNA and RNA. Viral nucleic acids were normalized to cellular nucleic acids for two purposes, to normalize for sample-to-sample variability in yield and to be able to relate viral RNA to viral DNA within each individual ganglion. Our first measurements of cellular DNA varied from 8.6 to 15 μg of DNA per sample (11.5 ± 2.1 μg per ganglion, $n = 28$, mean ± standard deviation SD, including mock- and virus-infected samples). After we changed methods from organic extraction to proteinase K digestion in subsequent experiments, we found that the cellular DNA amount was consistently higher (15.3 ± 0.7 μg per ganglion, $n = 36$, mean ± SD). Thus all viral DNA values were normalized to 15 μg of cellular DNA and expressed as "per ganglion." The amount of β-actin RNA expressed as $\log_{10}$ molecules per ganglion was 10.0 ± 0.4 ($\log_{10}$ mean ± SD, $n = 28$, including mock- and virus-infected samples). All viral RNA values were normalized to 10^{10} β-actin RNA molecules and expressed as "per ganglion."

RESULTS

Development of a QRPCR assay for HSV-1-specific RNAs in latently infected tissue. To ascertain whether there were HSV-1 productive-cycle transcripts present in latent infection in mice, we developed a sensitive PCR-based RNA assay for specific HSV-1 sequences and applied this assay to measure levels of transcripts arising from the IE gene, *ICP4*, the E gene, *tk*, and LATs. The principle of the assay was to compare the RNA-specific PCR signal of a virally infected tissue sample against a standard curve of known amounts of viral RNA. Figure 2 shows a flowchart of the assay. Mice were inoculated via corneal scarification, and 30 to 60 days later, trigeminal ganglia were rapidly harvested into liquid nitrogen. Each ganglion was transferred to GTC from liquid nitrogen and homogenized. One-tenth of this homogenate was used to prepare and analyze viral and cellular DNA. The remainder was used to prepare, purify, and analyze specific cellular and viral RNA sequences by comparison with standard curves of each gene sequence.

For a PCR assay to be quantitative, several criteria must be met (22). (i) The standards must be very close in composition to what is being tested. Relevant fragments of genes were cloned into transcription plasmids (Fig. 1), transcribed, quantified, and reconstituted with an amount and constitution of cellular RNA comparable to that of the trigeminal ganglion samples. (ii) Samples and standards must be prepared under identical conditions of reagent concentrations, enzyme activities, and times and temperatures of given reactions. Ganglionic and reconstituted standard RNAs were treated with DNase, purified by organic extraction, subjected to primer annealing, and reverse transcribed concomitantly, using the same reagents, enzyme lots, and conditions. (iii) PCR must remain in the linear range and sensitivity optimized with regard to primer selection, Mg^{2+} concentration, use of enhancing agents, and cycling parameters (times and temperatures of each step). Each assay was optimized initially using HSV DNA and then applied to cDNA derived from specific genes. Individual pa-

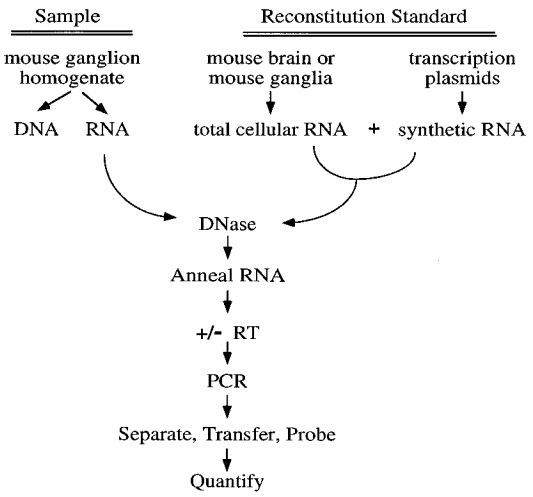

FIG. 2. QRPCR assay flowchart. After removal of an aliquot for DNA analysis, infected ganglion RNA and serial dilutions of synthetic standard RNA reconstituted in uninfected mouse brain RNA were assayed concomitantly as described in the text. Briefly, following DNase treatment, samples were reverse transcribed after a lengthy annealing time with a mixture of downstream (RNA-specific) primers, in the presence or absence of RT (+/− RT). Portions of the resulting cDNA were assayed by PCR for specific cellular and viral genes. PCR products were separated by acrylamide gel electrophoresis, transferred, probed with specific ^{32}P-end-labeled oligonucleotides, and quantified by using storage phosphor technology.

rameters are described in Materials and Methods. (iv) Quantitative assays require methods of detection which are sensitive, linear, and quantifiable. PCR products were probed with specific radiolabeled oligonucleotides and quantified by PhosphorImager analysis, which is as sensitive and reproducible as scintillation counting and has a linear range of 5 orders of magnitude (32). (v) The accuracy of a quantitative assay is determined by the reproducibility and variability of the measurement, which together define the quantitative limits of the assay. The assay for the IE gene, *ICP4*, is representative of our QRPCR approach. To ascertain the reproducibility of the assay for *ICP4*, transcription mixtures were prepared from stored stocks, diluted, reconstituted in 5 μg of total cellular mouse brain RNA, and assayed on two separate occasions. On the second occasion, the transcript dilutions were also reconstituted with total RNA made from individual uninfected mouse trigeminal ganglia to test whether any differences in RNA between these two nervous tissues would affect the assay. Products from these three standard curves were probed and quantified together. As shown in Fig. 3A, the assay was both very sensitive and highly reproducible. Plotted results of PhosphorImager quantification of these three standard curve comparisons (Fig. 3B) show that the assay was linear at this level of sensitivity on a log-log scale. QRPCR assays of the other gene sequences also generated linear, sensitive, and reproducible standard curves (see below). Because there was no demonstrable difference in the sensitivity or specificity of the *ICP4* signal, and because one animal provides more than 40 5-μg aliquots of brain RNA, all subsequent standard curves were reconstituted in brain RNA.

***ICP4*-specific RNA in latently infected ganglia.** The QRPCR assay was first applied to the *ICP4* gene because *ICP4* is an essential gene that is critically required for transcriptional activation of E and L genes (16, 53). To determine whether *ICP4* RNA was present, and at what level, in latently infected tissue, the QRPCR assay for *ICP4* was applied to mouse trigeminal

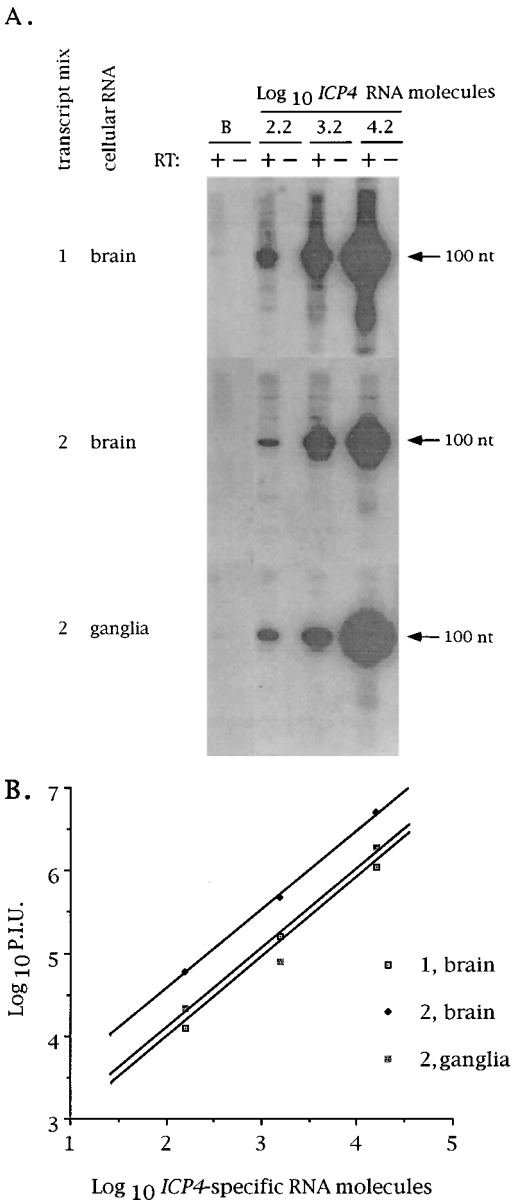

FIG. 3. Reproducibility of the QRPCR assay. (A) Autoradiographs of *ICP4* standard curves. Three standard reactions were assayed starting with 10-fold dilutions of two different synthetic transcript preparations (transcript mixes 1 and 2) and recombined with either uninfected mouse brain or mouse trigeminal ganglia RNA. The number of *ICP4* RNA molecules is expressed as $\log_{10}$; B represents a water blank mixed with cellular RNA. Standards prepared with (+) and without (−) RT are in adjacent lanes. The three standard sets were electrophoretically separated, transferred, and probed together for direct comparison. The 101-nt *ICP4*-specific product was verified by its migration similar to that of the 100-nt fragment (indicated on the right) of ϕX174 digested with *Hin*fI (not shown). Computer-generated images of this figure and Fig. 5, 7, and 8 were made from autoradiograms by using a Microtek ScanMaker II with Adobe Photoshop and Canvas software on a Macintosh IIci computer. (B) The radiolabeled blots of the standards shown in panel A were quantified by using storage phosphor technology, and the $\log_{10}$ values of PhosphorImager units (P.I.U.) were plotted against the $\log_{10}$ number of *ICP4* RNA molecules. The best-fit lines were generated by linear regression analysis.

ganglia latently infected with wild-type (wt) strain KOS or the *tk* mutant *dl*sptk at 30 days p.i. The *ICP4* signals were normalized to β-actin RNA measured simultaneously. As shown in Fig. 4 and Table 3 (experiment 1), an *ICP4*-specific RNA signal

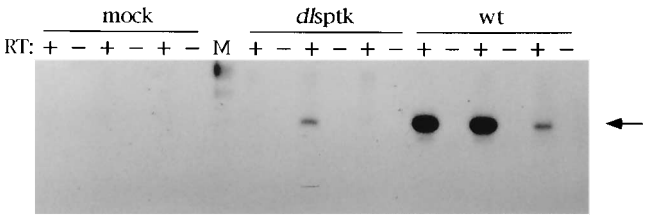

FIG. 4. *ICP4*-specific RNA in latently infected ganglia at 30 days p.i. An autoradiogram of a probed blot of *ICP4* QRPCR products separated on a 10% polyacrylamide gel is shown. Individual ganglion RNAs were reacted with (+) and without (−) RT and displayed in adjacent lanes. mock, three individual ganglia from animals inoculated with media not containing virus; *dl*sptk, three individual ganglia from animals inoculated with the *tk* deletion mutant *dl*sptk; wt, three individual ganglia from animals inoculated with wt strain KOS; M, molecular weight marker (ϕX174 digested with *Hin*fI and end labeled with ^{32}P). The 101-nt *ICP4*-specific signal (arrow) was detected by probing with oligonucleotide 4-3 and verified upon longer exposure of the molecular weight marker.

was detected in latently infected trigeminal ganglia (8 of 8 wt-infected ganglia and 3 of 10 *dl*sptk-infected ganglia) at a level of 1.6×10^2 to 2.5×10^4 molecules per ganglion. The absence of signal in the mock-infected controls demonstrates that the signal was virus specific. The absence of signal in the RT-negative controls demonstrates that the positive signal observed in the RT-containing lanes was RNA specific. Additionally, the PCR product was the predicted size for this primer pair, comigrated with those of both the transcript and DNA standards, and hybridized specifically with the oligonucleotide probe which is internal to the primers used to generate the product. Moreover, restriction digestion with *Hpa*II and *Bst*UI (not shown) yielded fragment patterns predicted from the published sequence (47) and comparable to restriction fragment patterns of the cDNA and DNA standards (39). These experiments show that RNA specific to *ICP4* is present in latently infected ganglia.

Variability of the *ICP4* signal relative to viral DNA. To examine the correlation of the *ICP4*-specific signal with the amount of viral DNA, we measured viral DNA and normalized it to cellular DNA by using PCR analysis of the mouse adipsin gene, a single-copy gene (33). We found that the *ICP4*-specific signal relative to viral DNA varied from 0.01 to 7 RNA molecules per viral genomes, or 700-fold (Table 3). Three of ten *dl*sptk-infected samples were positive for *ICP4*-specific RNA, and all had relatively high ratios of *ICP4*-specific RNA to viral DNA (1.2, 1.7, and 3.6), but because the amount of *dl*sptk DNA per ganglion was 1/10 that of wt DNA per ganglion (2.5 ± 0.3 [$n = 8$] versus 3.6 ± 0.6 [$n = 8$]; $\log_{10}$ mean ± SD, or 3.2×10^2 versus 4.0×10^3), the *dl*sptk samples in which no *ICP4*-specific RNA was detected may contain *ICP4*-specific RNA at levels below one copy per viral genome. These data show that the *ICP4*-specific RNA varied relative to viral DNA by nearly 3 orders of magnitude.

Constant level of LATs relative to viral DNA. To ascertain whether the large range of the RNA-to-DNA ratio measured for *ICP4* was specific to a productive-cycle gene in latent infection, we examined whether LATs relative to number of viral genomes had similar ranges of variabity. LATs were quantified in wt- and *dl*sptk-infected ganglia at 30 and 60 days p.i. (Fig. 5 and Table 4). The amount of viral DNA remained constant in wt-infected ganglia from 30 to 60 days p.i. (4.4 ± 0.3 [$n = 6$] versus 4.0 ± 0.2 [$n = 6$], $\log_{10}$ mean ± SD, or 2.5×10^4 versus 1.0×10^4). In *dl*sptk-infected ganglia, the amount of DNA was about 1 log unit lower but also remained constant from 30 to 60 days p.i. (3.5 ± 0.2 [$n = 7$] versus 3.7 ± 0.2 [$n = 8$], $\log_{10}$ mean ± SD, or 3.2×10^3 versus 5.0×10^3). The ratio of LAT to viral DNA was very consistent in both wt- and *dl*sptk-infected ganglia at 30 days (4.6 ± 0.4 [$n = 6$] versus 4.6 ± 0.4

TABLE 3. Viral DNA and *ICP4*-specific RNA content in latently infected mouse trigeminal ganglia at 30 and 60 days p.i.

Virus	30 days p.i.			60 days p.i.		
	DNA/TGG[a]	RNA/TGG[b]	RNA/DNA	DNA/TGG	RNA/TGG	RNA/DNA
Expt 1, wt (KOS)	4.8	3.0	0.01			
	3.6	4.4	6.9			
	3.1	3.9	6.6			
	3.7	2.9	0.1			
	2.8	2.4	0.4			
	3.3	2.4	0.1			
	3.5	2.9	0.3			
	3.7	2.2	0.03			
*dl*sptk	2.2	2.8	3.6			
	2.4	ND[c]				
	2.2	2.4	1.7			
	ND	ND				
	3.0	3.1	1.2			
	2.4	ND				
	ND	ND				
	2.8	ND				
	2.4	ND				
	2.6	ND				
Expt 2, wt (KOS)	4.6	2.7	0.01	4.3	2.7	0.02
	4.3	3.7	0.2	4.3	1.9	0.004
	4.3	3.6	0.2	3.9	2.3	0.02
	4.1	3.6	0.06	4.2	2.8	0.03
	4.8	3.3	0.2	3.7	4.2	3.2
	4.1	ND		3.9	4.1	1.6

[a] Viral DNA per trigeminal ganglion (TGG) normalized to 15 μg of cellular DNA ($\log_{10}$ molecules).
[b] *ICP4*-specific RNA per trigeminal ganglion normalized to 10^{10} molecules of β-actin RNA ($\log_{10}$ molecules).
[c] ND, not detected.

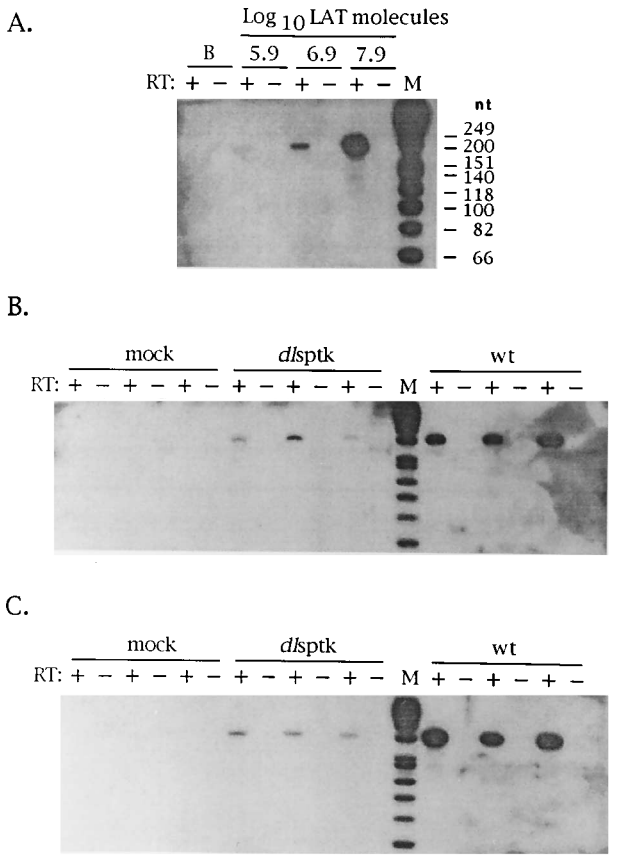

FIG. 5. LATs in latently infected ganglia at 30 and 60 days p.i. Autoradiograms of probed blots of LAT QRPCR products separated on 8% polyacrylamide gels are shown. Synthetic transcript mixes (A) or individual ganglion RNAs (B and C) were reacted with (+) and without (−) RT and displayed in adjacent lanes. (A) The LAT standard curve. The number of LAT molecules is expressed as $\log_{10}$; B represents a water blank mixed with cellular RNA. The size of the LAT-specific product was 195 nt. M, molecular weight marker as in Fig. 4, with fragment sizes indicated on the right. (B) LAT in latently infected ganglia at 30 days p.i. (C) LAT in latently infected ganglia at 60 days p.i. For definitions of mock, *dl*sptk, and wt, see the legend to Fig. 4. The 195-nt LAT-specific signal was detected by probing with oligonucleotide L-3.

[$n = 7$], $\log_{10}$ mean ± SD, or 4.0×10^4 each) and at 60 days (4.9 ± 0.2 [$n = 6$] versus 4.3 ± 0.4 [$n = 6$], $\log_{10}$ mean ± SD, or 7.9×10^4 versus 2.0×10^4). These data show that the ratio of LATs to viral DNA was constant.

***ICP4*-specific RNA at different times p.i.** We examined whether the presence of *ICP4*-specific RNA at 30 days p.i. represented RNA left over from the acute phase of ganglionic infection. This would imply a long half-life ($t_{1/2}$) in the context of latently infected tissue. Using a measured value of 10^8 molecules of *ICP4*-specific RNA per ganglion at 3 days p.i. (acute infection) (39) and the maximum value measured at 30 days, 2.5×10^4 molecules, we calculated a theoretical $t_{1/2}$ of about 5 days. This calculated $t_{1/2}$ predicts that no measurable *ICP4*-specific RNA would be present by 60 days p.i. To test this, animals inoculated at the same time were sacrificed at 30 and 60 days p.i. RNA was prepared immediately in each case and stored in ethanol at −80°C. After harvest at 60 days, both sets of samples were assayed together with appropriate standards. Figure 6 shows samples from each group. The *ICP4*-specific RNA values for all samples, normalized to 10^{10} β-actin molecules and to viral DNA normalized to 15 μg of cellular DNA, are compiled in Table 3 (experiment 2). These data show that

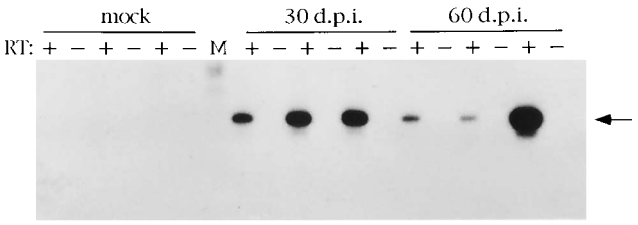

FIG. 6. *ICP4*-specific RNA in latently infected ganglia at 30 and 60 days p.i. (d.p.i.). An autoradiogram of a probed blot of *ICP4* QRPCR products separated on a 10% polyacrylamide gel is shown. Individual ganglion RNAs were reacted with (+) and without (−) RT and displayed in adjacent lanes. Six individual ganglia from animals infected with wt strain KOS are shown. mock, as in Fig. 4; M, molecular weight marker as in Fig. 4. The 101-nt *ICP4*-specific signal (arrow) was detected by probing with oligonucleotide 4-3 and verified as for Fig. 4.

both the absolute amounts and the ranges of *ICP4*-specific RNA were indistinguishable at 30 and 60 days p.i. Furthermore, the *ICP4*-specific RNA-to-viral DNA ratio ranged from 0.01 to 0.2 at 30 days p.i. and from 0.004 to 3.2 at 60 days p.i., values which overlap those obtained in experiment 1. Thus, the *ICP4*-specific RNA detected in latently infected ganglia does not appear to be attributable to a long RNA $t_{1/2}$.

Strand specificity of the ICP4 signal. LAT is transcribed downstream from and on the opposite strand of *ICP4* (Fig. 1A) and is transcribed in abundance during latency (14, 60, 66, 70) (Table 4). Because of the extreme sensitivity of the QRPCR assay and the reliance on heat denaturation of the RT without further purification, the possibility that the *ICP4* signal included a contribution from the opposite strand, especially from LAT run-on transcription, was examined. For amplification of the complementary strand prior to or concomitant with the PCR, two conditions would be required: there would have to be residual RT activity after the heat denaturation step, and there would have to be antisense RNA present in sufficient abundance to be reverse transcribed under suboptimal reaction conditions of enzyme activity, time, temperature, and composition. *ICP4* antisense transcripts were generated and quantified. In a reconstruction experiment, *ICP4* antisense transcripts at a molar excess of 10^5-fold antisense to sense transcripts did not contribute to the *ICP4* signal (39). In addition, we tested whether *ICP4*-specific RNA was present in ganglia infected with a mutant which is severely impaired for expression of LATs. In this experiment, mice were mock infected or infected with wt virus or the LAT promoter mutant *dl*LAT1.8 (43) and harvested at 30 days p.i. As shown in Fig. 7A, the *ICP4*-specific RNA sense signal was detected in *dl*-LAT1.8 latently infected ganglia, and the amount per ganglion and per viral DNA was no less than that found in wt-infected ganglia (Table 5). We conclude that the *ICP4*-specific RNA signal detected in our assay was strand specific.

Does the *ICP4*-specific RNA detected in latently infected tissue initiate at the *ICP4* promoter? The finding of RNA specific to the *ICP4* gene in latently infected ganglia raises the possibility of authentic ICP4 expression during latency. To begin to address this possibility, we examined whether any of the *ICP4*-specific RNA that we observed in latently infected ganglia was consistent with utilization of the *ICP4* promoter. We devised a coamplification PCR assay, using one common downstream primer and two upstream primers, one within and one upstream of the *ICP4* transcription start site utilized during productive infection (59). As depicted in Fig. 1C, amplification of DNA would generate two products of 101 and 184 nucleotides (nt) in length, while amplification of RNA initiating at the *ICP4* promoter would yield only the shorter product.

Coamplification was possible from both HSV DNA and cDNA made from the transcription standard (Fig. 8). This assay was applied to three 30-day-p.i. wt-infected ganglion samples in which an *ICP4*-specific RNA signal had been measured. In two of the samples, both the 101- and 184-nt products were present. The 184-nt product shows that RNA initiating upstream of the *ICP4* promoter was present, while the 101-nt product could correspond to either RNA initiating at the *ICP4* promoter or RNA initiating upstream from the *ICP4* promoter or both. In one of three samples tested, the signal included only the 101-nt product, consistent with initiation at the *ICP4* promoter. This finding provides evidence that in latency, *ICP4* promoter-specific initiation of the *ICP4*-specific RNA can occur in the absence of read-through transcription.

Correlation of *ICP4*-specific and *tk*-specific RNA in latently infected tissue. E genes, such as *tk*, are targets for ICP4 transactivation (16, 53). We applied the QRPCR assay for *tk* to determine whether any *tk*-specific RNA could be measured in latently infected ganglia RNA and by measuring *ICP4*-specific RNA in the same samples to determine if there was a correlation. The *tk* assay was less sensitive than the assay for *ICP4*, probably because of a combination of lower efficiencies in reverse transcription and PCR amplification. In addition, we occasionally encountered the presence of a low-level positive signal in the RT-minus reactions. When compared with the DNA standard curve, the positive signal indicated contamination at the level of single molecules of DNA. This was possibly due to PCR product carryover or incomplete DNase digestion of viral genomic DNA in the RNA preparation. As shown in Fig. 7B and Table 5, we did detect *tk*-specific RNA in ganglia at 30 days p.i. at a level up to 500 molecules per viral genome. By comparing Fig. 7A with Fig. 7B, a correlation between the two can be seen. Linear regression analysis applied to the quantified normalized values generated the following relationship: $\log_{10}$ *tk* = 3.0 + 0.68 $\log_{10}$ *ICP4*; r^2 = 0.79 (Fig. 7C). These results show that the amount of *tk*-specific RNA and *ICP4*-specific RNA correlated in latently infected mouse trigeminal ganglia over a 2-log-unit range.

DISCUSSION

We have developed a PCR-based assay for detection and quantification of selected HSV-1 transcripts from individual mouse ganglia. We found that (i) *ICP4*-specific RNA of the correct strand is present in latent infection at 30 and 60 days p.i., (ii) some of the *ICP4*-specific RNA initiates in a region that is consistent with the *ICP4* promoter, (iii) *ICP4*-specific RNA expression fluctuates widely from ganglion to ganglion, (iv) *tk*-specific RNA is also present in latent infection, and (v) a correlation is seen between the *ICP4*-specific and the *tk*-specific RNAs. We discuss the assay that we used and the potential significance of our findings for gene expression during latency.

Parameters of the QRPCR assay. We chose to develop a QRPCR assay with external standards rather than utilize a competitive strategy such as that used by Ramakrishnan et al. (57). Either method is capable of great sensitivity, but the competitive approach requires dividing each sample into many portions to quantify a single gene sequence, while the external standard approach permits dividing each sample into several portions for measurement of many different gene sequences and therefore yields more information per individual sample. Essential factors in the success of the assay included maximizing RNA recovery, sensitivity, and specificity. To maximize RNA recovery, we rapidly collected tissue into liquid nitrogen and used the GTC-CsCl method. We assayed the 5′ ends of target RNAs to hedge against 3′-to-5′ exonuclease degradation. To maximize sensitivity, we used a long annealing time for priming reverse transcription to permit hybridization with rare RNA. In our hands, sensitivity was improved over 10-fold by using specific primers rather than random primers (48). Reconstituting synthetic RNA standards with cellular RNA controlled for nonspecific amplification of and/or competition by cellular sequences. Use of a radiolabeled probe maximized detection of a specific PCR product. We used mock-infected and RT-negative samples to control for contamination. We conclude that RNA containing the sequence which this assay amplifies is present in latently infected tissue.

Is *ICP4* RNA transcribed during latency? Although we clearly detect RNA specific to the *ICP4* gene during latency, our results do not permit us to conclude that these transcripts are identical to the *ICP4* mRNA prevalent in productively infected cells. Three results, however, point in that direction: (i) the RNA is the correct polarity, (ii) in at least some of the ganglia, it appears to initiate in a manner consistent with uti-

TABLE 4. Viral DNA and LAT content in latently infected mouse trigeminal ganglia at 30 and 60 days p.i.

Virus	30 days p.i.			60 days p.i.		
	DNA/TGG[a]	LATs/TGG[b]	LATs/DNA[c]	DNA/TGG	LATs/TGG	LATs/DNA
*dl*sptk	3.3	8.5	5.2	3.2	8.2	5.0
	3.6	7.8	4.1	3.5	8.1	4.6
	3.8	8.1	4.3	4.0	7.8	3.8
	3.5	8.4	4.9	3.8	7.7	3.9
	3.4	7.7	4.3	3.8	8.1	4.3
	3.3	8.2	4.9	3.6	7.9	4.3
	ND[d]	8.0		3.7	8.2	4.5
	3.1	7.8	4.7	3.8	8.0	4.2
wt (KOS)	4.6	8.6	4.0	4.3	9.2	4.9
	4.3	8.8	4.5	4.3	9.0	4.7
	4.3	9.1	4.8	3.9	8.8	4.9
	4.1	8.9	4.8	4.2	8.9	4.7
	4.8	9.2	4.4	3.7	8.8	5.1
	4.1	9.4	5.3	3.9	9.0	5.1

[a] Viral DNA per trigeminal ganglion (TGG) normalized to 15 μg of cellular DNA ($\log_{10}$ molecules).
[b] LATs per trigeminal ganglion normalized to 10^{10} molecules of β-actin RNA ($\log_{10}$ molecules).
[c] Ratio expressed in $\log_{10}$.
[d] ND, not detected.

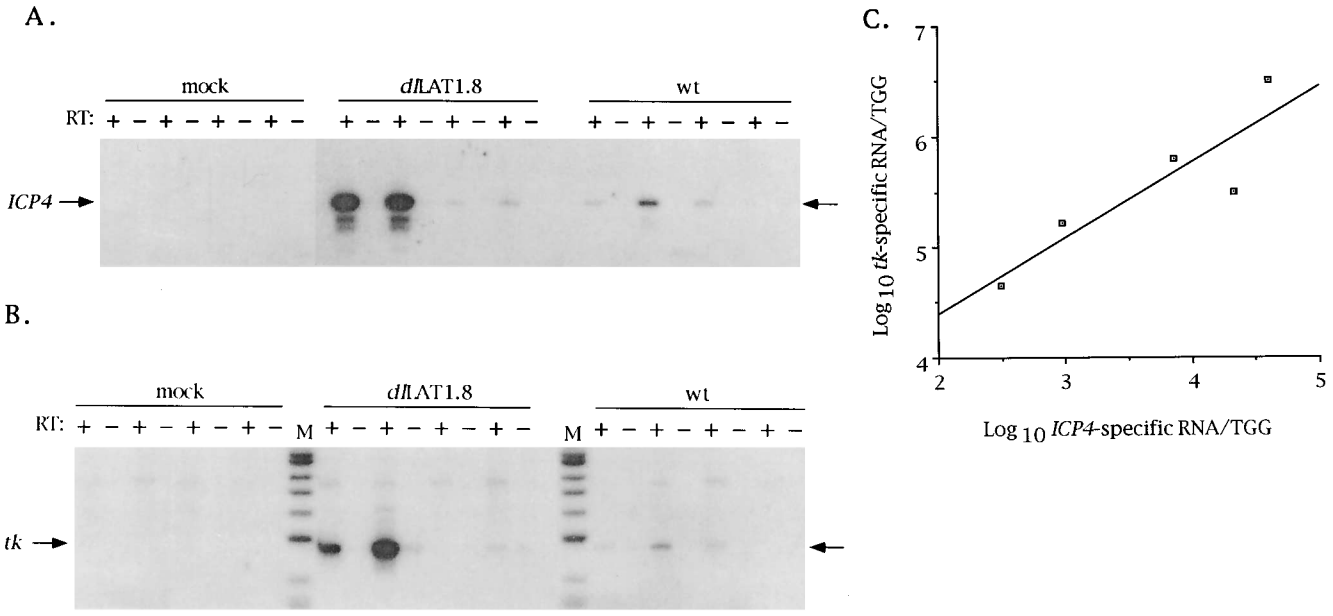

FIG. 7. Strand specificity and correlation of expression of *ICP4*-specific RNA and *tk*-specific RNA in ganglia latently infected with wt or *dl*LAT1.8. (A and B) Autoradiograms of probed blots of QRPCR products separated on 10% (A) and 12% (B) polyacrylamide gels. Individual ganglion RNAs were reacted with (+) and without (−) RT and displayed in adjacent lanes. (A) *ICP4*-specific RNA. The 101-nt *ICP4*-specific product (arrow) was detected by probing with oligonucleotide 4-3 and verified as for Fig. 4 (molecular weight marker not shown). (B) *tk*-specific RNA from the samples shown in panel A. The 60-nt *tk*-specific product (arrow) was detected by probing with oligonucleotide tk-3. M, molecular weight marker as in Fig. 4; mock and wt, as in Fig. 4; *dl*LAT1.8, individual ganglia from animals inoculated with the LAT promoter deletion mutant *dl*LAT1.8 (43). In some RT− lanes, signal was detected at a level which was always less than 10% that detected in the corresponding RT+ lanes. Higher-molecular-weight bands seen in the RT+ lanes are present in mock-infected and virus-infected samples and comigrate with a band visible by ethidium bromide staining; thus, they represent abundant products arising from cellular sequences and exhibiting weak complementarity to the *tk*-specific probe. (C) *tk*-specific RNA per trigeminal ganglion (TGG) plotted against *ICP4*-specific RNA per trigeminal ganglion, both normalized to β-actin RNA as described in the text and expressed in $\log_{10}$ (data from Table 5; best-fit plotted line generated by linear regression of $\log_{10}$ values).

lization of the *ICP4* promoter, and (iii) its expression positively correlates with expression of *tk*-specific RNA.

In certain ganglia, some of the *ICP4*-specific transcripts initiate upstream of the *ICP4* promoter. These transcripts might conceivably correspond to RNA detected in productively infected cells (27), which is 3′ coterminal with ICP4 and of the E kinetic class.

A second issue is whether these transcripts arise from de novo transcription during latency. Our results comparing transcript levels at 3, 30, and 60 days p.i. (Fig. 6 and reference 39) argue against these RNAs merely being carried over from acute infection. Additionally, we find substantial amounts of *ICP4*-specific RNA in ganglia latently infected with *dl*sptk, which does not abundantly express *ICP4* RNA during acute ganglionic infection (36, 39). Assuming, then, that the *ICP4*-specific RNA is the product of transcription during latency, the issue becomes whether its existence represents transcriptional noise, i.e., very low level, possibly nonspecific transcriptional events. This is especially possible in those ganglia in which the ratio of *ICP4*-specific RNA to DNA is very low (<0.1). However, it is difficult to invoke noise to explain the ~20% of ganglia in which the ratio is fairly high (>1), especially considering that this RNA signal could be derived from one or a few cells. Given a value of about 100 to 200 latently infected cells per mouse trigeminal ganglion infected with HSV-1 KOS or KOS(M) via corneal scarification, as measured by reporter gene (*lacZ*) expression of β-galactosidase (13, 62) or by LAT in situ hybridization analysis (38), and our viral DNA values (Tables 3 to 5), we can estimate a copy number of about 100 viral genomes per infected cell. If the *ICP4*-specific RNA is derived from a single cell, the ratio of *ICP4* transcripts to viral genomes could be >100.

If *ICP4* RNA is transcribed during latency, is active protein expressed? Our assay permits measurement of transcripts for several genes from the same sample. We chose to assay for *tk* because *tk* transcription is dependent upon ICP4 activation. ICP4 induces a 30-fold increase in *tk* RNA expression in the context of productive infection (29, 30). There was a strong positive correlation ($r = 0.79$) between the amounts of *ICP4*-specific and *tk*-specific RNAs. Interpretations of this correlation include the following: (i) there is a casual relationship

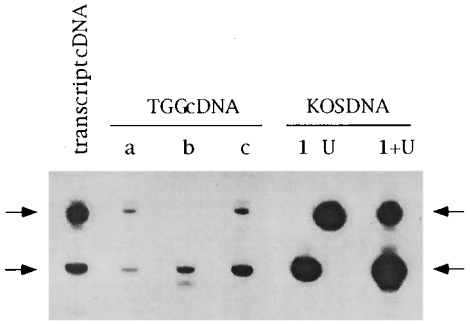

FIG. 8. Assay to determine the 5′ limit of *ICP4*-specific RNA detected in latently infected ganglia. Coamplification of longer (184 nt; upper arrows) and shorter (101 nt; lower arrows) PCR products with a common downstream primer (4-2) and two upstream primers, one situated 5′ of the transcript start site (4-U) and the other situated within the 5′ mRNA leader region (4-1), as diagramed in Fig. 1C. Lanes from the left: coamplification using plasmid pKS+5′ICP4 derived cDNA; coamplification of cDNA from three individual latently infected trigeminal ganglia (TGG), a, b, and c; amplification of KOS strain HSV DNA with 4-2 and only 4-1 (1), only 4-U (U), or both (1+U).

TABLE 5. Viral DNA and *ICP4*-specific and *tk*-specific RNA content in latently infected mouse trigeminal ganglia at 30 days p.i.

Virus	DNA/TGG[a]	*ICP4*		*tk*		*tk*/*ICP4*
		RNA/TGG[b]	RNA/DNA	RNA/TGG[b]	RNA/DNA	
wt (KOS)	3.7	3.0	0.2	5.2	33	160
	4.1	3.9	0.6	5.8	49	79
	3.8	2.5	0.05	4.6	7	130
	3.1	ND[c]		ND		
*dl*LAT1.8	4.4	4.3	0.8	5.5	13	16
	3.8	4.6	6.3	6.5	510	79
	3.8	2.2	0.03	ND		
	3.9	2.4	0.04	ND		

[a] Viral DNA per trigeminal ganglion (TGG) normalized to 15 μg of cellular DNA ($\log_{10}$ molecules).
[b] HSV-specific RNA per trigeminal ganglion normalized to 10^{10} molecules of β-actin RNA ($\log_{10}$ molecules).
[c] ND, not detected.

(that is, the *ICP4*-specific RNA encodes a protein that induces *tk*-specific RNA expression) and (ii) the levels of transcript accumulation are higher in the same ganglia because of some general increase in transcriptional activity. Although we cannot rule out the second interpretation, it is interesting to entertain the first. If there is a causal relationship, it could occur throughout the particular ganglia, resulting from a global signal, or it could occur in one or a few latently infected cells. Is the measured amount of *ICP4*-specific RNA sufficient for physiologic activity? We think that it is, in particular if only one or a few cells account for most of the signal. If only one or a few cells contain most of the *ICP4*-specific RNA, then there could be up to 4×10^4 *ICP4*-specific RNA molecules in that latently infected cell, which is probably sufficient for physiologically relevant ICP4 expression and activity.

A third intrepretation for the finding of *ICP4*-specific RNA in latency is that ICP4 plays a role in maintaining latency as a result of its ability to transrepress IE genes (50) or regulate LATs (58). However the correlation of *ICP4*-specific RNA with *tk*-specific RNA tends to argue against this interpretation. We favor the hypothesis that transient or low-frequency expression of ICP4 leads to E gene transcription in some proportion of latently infected ganglia.

If active ICP4 protein is expressed during latency, does this imply low-level viral replication? Our results raise this possibility. In the natural human host and in animal models which exhibit spontaneous reactivation, replication in neurons presumably precedes appearance of virus in that replication-dependent L genes encode virion components. ICP4 antigen has been detected in latently infected rabbit ganglia (25), and the rabbit model is known to exhibit spontaneous reactivation (40). However, the published record provides no evidence for replication or spontaneous reactivation in mice. In our model system, CD-1 mice, infection with KOS or another virus with wt growth and reactivation characteristics, 0 of 18 ganglia contained infectious virus at the time of explant at 28 days p.i. (42). We compared quantitative measurements from various reports, limited to mouse trigeminal ganglia infected via corneal scarification but including several virus strains and mouse strains. In a total of 131 ganglia, no infectious virus was found at the time of explant, which was from 11 to 115 days p.i. (41, 49, 63, 75). Other reports in which the number of negative controls was not stated document the same negative result (15, 19, 65, 66, 67). To determine whether low-level infectious virus was present but not detected by plaque assay because of physical entrapment by some cellular or tissue component, we performed the following test. Fifty PFU of wt virus was mixed with uninfected trigeminal ganglia tissue homogenates before or after freeze-thawing and sonication; we recovered similar numbers of PFU under all conditions (39). This result shows that physical association of virus with cellular components made accessible by tissue disruption does not prevent detection of infectious virus by plaque assay. However, mixing extracellular virus with tissue homogenate is not identical to intracellular virus released by homogenization, so very low frequency reactivation may remain undetected by plaque assay of ganglionic homogenates. In addition, a recent report raises the possibility that noninfectious nucleocapsids are axonally transported separately from glycoproteins and enveloped in distal regions of the axon (51).

HSV maintains divergent goals of preserving latency while permitting low-frequency reactivation. As discussed by Hill (26), the operational definition of reactivation is the detection of infectious virus from latently infected tissue. The process whereby a stably latent viral genome generates an infectious particle is not known. Investigators generally acknowledge that complex host and viral features regulate latency and reactivation. Some have discussed reactivation as the inevitable consequence of a single event, a switch, invoking the lytic cascade of IE, E, and L genes as resulting from the triggering of such a switch (63, 70, 78). In the context of latent infection, it has been suggested that IE gene expression may constitute a switch initiating the lytic cascade leading to reactivation (34, 45, 48). A cascade is a series of reactions whereby each reaction is necessary and sufficient for, and may augment, the subsequent reaction. In contrast, Kosz-Vnenchak et al. (37) proposed that reactivation requires more than turning on IE genes, and Bloom et al. (4) addressed the possibility that reactivation occurs in stages. We suggest that the process of reactivation is more of an uphill climb than the downhill process suggested by the word "cascade." Each specific step of expression of viral components would be necessary but not sufficient for progress to the subsequent step. Progress from one step to the next would occur only at some low frequency. The following scenario is offered to illustrate this suggestion. (i) Most latently infected ganglia contain various low levels of virus-specific RNAs other than LATs, for example as shown in this report, but do not express sufficient IE RNA to generate physiologically relevant levels of protein. (ii) A percentage of latently infected cells are perturbed in some manner, such as through trophic factor signalling pathways (64) or metabolic insults (21, 41, 72), to express specific IE proteins which can transactivate E genes to a limited extent. (iii) A percentage of cells containing some E RNAs accumulate sufficient relative amounts of all necessary E proteins to threshold levels to permit limited replication. Host-specific (4, 57), tissue-specific (67), cell-type-specific (34, 45, 46, 76), and virus strain-specific (24) factors may affect the kinetics of any intermediate step. For example,

step iii, limited replication, may be permitted at a much lower frequency in mice than in humans. (iv) Once limited replication ensues, a replication-dependent viral function may upregulate IE expression, leading to the lytic cascade and production of viral particles, as suggested by Kosz-Vnenchak et al. (36, 37). Such a function may be an L gene or it may be that replication alters the nucleosome-associated DNA (18) in a manner which alters the program of gene expression (79). Early steps in replication as well as subsequent steps such as axonal transport and peripheral infection may be subject to broader host controls, such as the immunologic state. Thus, the kinetic pattern of the HSV replication cycle may be viewed as series of steps mounting to reactivation rather than as a downhill cascade in the context of infection of nervous tissue.

ACKNOWLEDGMENTS

We thank David Knipe, Magdalena Kosz-Vnenchak, and David Leib for communicating unpublished results; Shigeru Sakiyama for providing plasmid pSPMβA1; David Knipe for providing plasmid pK1-2; Charles Hwang for providing plasmid pSVtk; Priscilla Schaffer for providing plasmid pRFS and HSV mutant *dl*LAT1.8; Jennie Jacobson for advice on animal protocols; Paul Digard and Charles Hwang for helpful discussions on transcription; Ethan Bodin for initial work in QRPCR; and Lynda Morrison for invaluable discussions on viral latency. We thank Larry Feldman for suggestions which led to the LAT^- and antisense experiments. David Knipe is especially appreciated for critical review of the manuscript.

This research was supported by NIH grant PO1 AI24010. M.F.K. was supported in part by a fellowship from the Albert J. Ryan Foundation.

REFERENCES

1. **Arrigo, S. J., S. Weitsman, J. D. Rosenblatt, and I. S. Y. Chen.** 1989. Analysis of *rev* gene function on human immunodeficiency virus type 1 replication in lymphoid cells by using a quantitative polymerase chain reaction method. J. Virol. **63:**4875–4881.
2. **Ausubel, F. M., R. Brent, R. E. Kingston, D. D. Moore, J. A. Smith, J. G. Seidman, and K. Struhl (ed.).** 1994. Current protocols in molecular biology. John Wiley & Sons, Inc., New York.
3. **Baringer, J. R., and P. Swoveland.** 1973. Recovery of herpes-simplex virus from human trigeminal ganglions. N. Engl. J. Med. **288:**648–650.
4. **Bloom, D. C., G. B. Devi-Rao, J. M. Hill, J. G. Stevens, and E. K. Wagner.** 1994. Molecular analysis of herpes simplex virus type 1 during epinephrine-induced reactivation of latently infected rabbits in vivo. J. Virol. **68:**1283–1292.
5. **Chirgwin, J. J., A. E. Przybyla, R. J. MacDonald, and W. J. Rutter.** 1979. Isolation of biologically active ribonucleic acid from sources enriched in ribonuclease. Biochemistry **18:**5294–5299.
6. **Chou, Q., M. Russell, D. E. Birch, J. Raymond, and W. Bloch.** 1992. Prevention of pre-PCR mis-priming and primer dimerization improves low-copy-number amplifications. Nucleic Acids Res. **20:**1717.
7. **Coen, D. M., H. E. Fleming, Jr., L. K. Leslie, and M. J. Retondo.** 1985. Sensitivity of arabinosyladenine-resistant mutants of herpes simplex virus to other antiviral drugs and mapping of drug hypersensitivity mutations to the DNA polymerase locus. J. Virol. **53:**477–488.
8. **Coen, D. M., M. Kosz-Vnenchak, J. G. Jacobson, D. A. Leib, C. L. Bogard, P. A. Schaffer, K. L. Tyler, and D. M. Knipe.** 1989. Thymidine kinase-negative herpes simplex virus mutants establish latency in mouse trigeminal ganglia but do not reactivate. Proc. Natl. Acad. Sci. USA **86:**4736–4740.
9. **Cook, M. L., V. B. Bastone, and J. G. Stevens.** 1974. Evidence that neurons harbor latent herpes simplex virus. Infect. Immun. **9:**946–951.
10. **Croen, K. D., J. M. Ostrove, L. Dragovic, and S. E. Straus.** 1991. Characterization of herpes simplex virus type 2 latency-associated transcription in human sacral ganglia and in cell culture. J. Infect. Dis. **163:**22–28.
11. **Croen, K. D., J. M. Ostrove, L. J. Dragovic, J. E. Smialek, and S. E. Straus.** 1987. Latent herpes simplex virus in human trigeminal ganglia: detection of an immediate early gene "anti-sense" transcript by in situ hybridization. N. Engl. J. Med. **317:**1427–1431.
12. **Croen, K. D., J. M. Ostrove, L. J. Dragovic, and S. E. Straus.** 1988. Patterns of gene expression and sites of latency in human nerve ganglia are different for varicella-zoster and herpes simplex viruses. Proc. Natl. Acad. Sci. USA **85:**9773–9777.
13. **Davar, G., M. F. Kramer, D. Garber, A. L. Roca, J. K. Andersen, W. Bebrin, D. M. Coen, M. Kosz-Vnenchak, D. M. Knipe, X. O. Breakefield, and O. Isacson.** 1994. Comparative efficacy of expression of genes delivered to mouse sensory neurons with herpes virus vectors. J. Comp. Neurol. **393:**3–11.
14. **Deatly, A. M., J. G. Spivack, E. Lavi, and N. W. Fraser.** 1987. RNA from an immediate early region of the type 1 herpes simplex virus genome is present in the trigeminal ganglia of latently infected mice. Proc. Natl. Acad. Sci. USA **84:**3204–3208.
15. **Deatly, A. M., J. G. Spivak, E. Lavi, D. R. O'Boyle II, and N. W. Fraser.** 1988. Latent herpes simplex virus type 1 transcripts in peripheral and central nervous system tissues of mice map to similar regions of the viral genome. J. Virol. **62:**749–756.
16. **DeLuca, N. A., A. McCarthy, and P. A. Schaffer.** 1985. Isolation and characterization of deletion mutants of herpes simplex virus type 1 in the gene encoding immediate-early regulatory protein ICP4. J. Virol. **56:**558–570.
17. **DeLuca, N. A., and P. A. Schaffer.** 1987. Activities of herpes simplex virus type 1 (HSV-1) ICP4 genes specifying nonsense peptides. Nucleic Acids Res. **15:**4491–4510.
18. **Deshmane, S. L., and N. W. Fraser.** 1989. During latency, herpes simplex virus type 1 DNA is associated with nucleosomes in a chromatin structure. J. Virol. **63:**943–947.
19. **Devi-Rao, G. B., D. C. Bloom, J. G. Stevens, and E. K. Wagner.** 1994. Herpes simplex type 1 DNA replication and gene expression during explant-induced reactivation of latently infected murine sensory ganglia. J. Virol. **68:**1271–1282.
20. **Ecob-Prince, M. S., F. J. Rixon, C. M. Preston, K. Hassan, and P. G. E. Kennedy.** 1993. Reactivation in vivo and in vitro of herpes simplex virus from mouse dorsal root ganglia which contain different levels of latency-associated transcripts. J. Gen. Virol. **74:**995–1002.
21. **Fawl, R. L., and B. Roizman.** 1993. Induction of reactivation of herpes simplex virus in murine sensory ganglia in vivo by cadmium. J. Virol. **67:**7025–7031.
22. **Ferre, F.** 1992. Quantitative or semi-quantitative PCR: reality versus myth. PCR Methods Appl. **2:**1–9.
23. **Gordon, Y. J., B. Johnson, E. Romanowski, and T. Araullo-Cruz.** 1988. RNA complementary to herpes simplex virus type 1 ICP0 gene demonstrated in neurons of human trigeminal ganglia. J. Virol. **62:**1832–1835.
24. **Gordon, Y. J., J. L. C. McKnight, J. M. Ostrove, E. Romanowski, and T. Araullo-Cruz.** 1990. Host species and strain differences affect the ability of an HSV-1 ICP0 deletion mutant to establish latency and spontaneously reactivate *in vivo*. Virology **178:**469–477.
25. **Green, M. T., R. J. Courtney, and E. C. Dunkel.** 1981. Detection of an immediate early herpes simplex virus type 1 polypeptide in trigeminal ganglia from latently infected animals. Infect. Immun. **34:**987–992.
26. **Hill, T. J.** 1982. Herpes simplex virus latency, p. 175–240. *In* B. Roizman (ed.), The herpesviruses, vol. 3. Plenum, New York.
27. **Hubenthal-Voss, J., L. Starr, and B. Roizman.** 1987. The herpes simplex virus origins of DNA synthesis in the S component are each contained in a transcribed open reading frame. J. Virol. **61:**3349–3355.
28. **Hwang, C. B. C., B. Horsburgh, E. Pelosi, S. Roberts, P. Digard, and D. M. Coen.** 1994. A net +1 frameshift permits synthesis of thymidine kinase from a drug-resistant herpes simplex virus mutant. Proc. Natl. Acad. Sci. USA **91:**5461–5465.
29. **Imbalzano, A. N., D. M. Coen, and N. A. DeLuca.** 1991. Herpes simplex virus transactivator ICP4 operationally substitutes for the cellular transcription factor Sp1 for efficient expression of the viral thymidine kinase gene. J. Virol. **65:**565–574.
30. **Imbalzano, A. N., and N. A. DeLuca.** 1992. Substitution of a TATA box from a herpes simplex virus late gene in the viral thymidine kinase promoter alters ICP4 inducibility but not temporal expression. J. Virol. **66:**5453–5463.
31. **Irmiere, A. F., M. M. Manos, J. G. Jacobson, J. S. Gibbs, and D. M. Coen.** 1989. Effect of an amber mutation in the herpes simplex virus thymidine kinase gene on polypeptide synthesis and stability. Virology **168:**210–220.
32. **Johnston, R. F., S. C. Pickett, and D. L. Barker.** 1990. Autoradiography using storage phosphor technology. Electrophoresis **11:**355–360.
33. **Katz, J. P., E. T. Bodin, and D. M. Coen.** 1990. Quantitative polymerase chain reaction analysis of herpes simplex virus DNA in ganglia of mice infected with replication-incompetent mutants. J. Virol. **64:**4288–4295.
34. **Kemp, L. M., and D. S. Latchman.** 1989. Regulated transcription of herpes simplex virus immediate-early genes in neuroblastoma cells. Virology **171:**607–610.
35. **Knotts, F. B., M. L. Cook, and J. G. Stevens.** 1974. Pathogenesis of herpetic encephalitis in mice after ophthalmic inoculation. J. Infect. Dis. **130:**16–27.
36. **Kosz-Vnenchak, M., D. M. Coen, and D. M. Knipe.** 1990. Restricted expression of herpes simplex virus lytic genes during establishment of latent infection by thymidine kinase-negative mutant viruses. J. Virol. **64:**5396–5402.
37. **Kosz-Vnenchak, M., J. Jacobson, D. M. Coen, and D. M. Knipe.** 1993. Evidence for a novel regulatory pathway for herpes simplex virus gene expression in trigeminal ganglion neurons. J. Virol. **67:**5383–5393.
38. **Kosz-Vnenchak, M., and D. M. Knipe (Harvard Medical School).** 1994. Personal communication.
39. **Kramer, M. F., and D. M. Coen.** 1994. Unpublished observations.
40. **Laibson, P. R., and S. Kibrick.** 1969. Recurrence of herpes simplex virus in rabbit eyes: results of a three-year study. Invest. Ophthalmol. **8:**346–350.
41. **Laycock, K. A., S. F. Lee, R. H. Brady, and J. S. Pepose.** 1991. Character-

ization of a murine model of recurrent herpes simplex viral keratitis induced by ultraviolet B radiation. Invest. Ophthalmol. Visual Sci. **32:**2741–2746.
42. **Leib, D. A. (Washington University).** 1994. Personal communication.
43. **Leib, D. A., C. L. Bogard, M. Kosz-Vnenchak, K. A. Hicks, D. M. Coen, D. M. Knipe, and P. A. Schaffer.** 1989. A deletion mutant of the latency-associated transcript of herpes simplex virus type 1 reactivates from the latent state with reduced frequency. J. Virol. **63:**2893–2900.
44. **Leib, D. A., D. M. Coen, C. L. Bogard, K. A. Hicks, D. R. Yager, D. M. Knipe, K. L. Tyler, and P. A. Schaffer.** 1989. Immediate-early regulatory gene mutants define different stages in the establishment and reactivation of herpes simplex virus latency. J. Virol. **63:**759–768.
45. **Lillycrop, K. A., M. K. Howard, J. K. Estridge, and D. S. Latchman.** 1994. Inhibition of herpes simplex virus infection by ectopic expression of neuronal splice variants of the Oct-2 transcription factor. Nucleic Acids Res. **22:**815–820.
46. **Margolis, T. P., F. Sedarati, A. T. Dobson, L. T. Feldman, and J. G. Stevens.** 1992. Pathways of viral gene expression during acute neuronal infection with HSV-1. Virology **189:**150–160.
47. **McGeogh, D. J., A. Dolan, S. Donald, and D. H. K. Brauer.** 1986. Complete DNA sequence of the short repeat region in the genome of herpes simplex virus type 1. Nucleic Acids Res. **14:**1727–1743.
48. **Minagawa, H., S. Tanaka, Y. Toh, and R. Mori.** 1994. Detection of herpes simplex virus type 1-encoded RNA by polymerase chain reaction: different pattern of viral RNA detection in latently infected murine trigeminal ganglia following *in vitro* or *in vivo* reactivation. J. Gen. Virol. **75:**647–650.
49. **Mitchell, W. J., P. Gressens, J. R. Martin, and R. DeSanto.** 1994. Herpes simplex virus type 1 DNA persistence, progressive disease and transgenic immediate early gene promoter activity in chronic corneal infections in mice. J. Gen. Virol. **75:**1201–1201.
50. **O'Hare, P., and G. S. Hayward.** 1985. Three *trans*-acting regulatory proteins of herpes simplex virus modulate immediate-early gene expression in a pathway involving positive and negative feedback regulation. J. Virol. **56:** 723–733.
51. **Penfold, M. E., P. Armati, and A. L. Cunningham.** 1994. Axonal transport of herpes simplex virions to epidermal cells: evidence for a specialized mode of virus transport and assembly. Proc. Natl. Acad. Sci. USA **91:**6529–6533.
52. **Pepose, J. S., R. Y. Foos, and J. G. Stevens.** 1986. Herpes simplex virus immediate-early protein ICP4 in murine models of latency. Graefe's Arch. Clin. Exp. Ophthalmol. **224:**341–345.
53. **Preston, C. M.** 1979. Control of herpes simplex virus type 1 mRNA synthesis in cells infected with wild-type virus of the temperature-sensitive mutant *tsK*. J. Virol. **29:**275–284.
54. **Promega Corporation.** 1991. Protocols and applications guide, 2nd ed. Promega Corporation, Madison, Wis.
55. **Puga, A., and A. L. Notkins.** 1987. Continued expression of a poly(A)$^+$ transcript of herpes simplex virus type 1 in trigeminal ganglia of latently infected mice. J. Virol. **61:**1700–1703.
56. **Puga, A., J. D. Rosenthal, H. Openshaw, and A. L. Notkins.** 1978. Herpes simplex virus DNA and mRNA sequences in acutely and chronically infected trigeminal ganglia of mice. Virology **89:**102–111.
57. **Ramakrishnan, R., D. J. Fink, G. Jiang, P. Desai, J. C. Glorioso, and M. Levine.** 1994. Competitive quantitative PCR analysis of herpes simplex virus type 1 DNA and latency-associated transcript RNA in latently infected cells of the rat brain. J. Virol. **68:**1864–1873.
58. **Rivera-Gonzalez, R., A. N. Imbalzano, B. Gu, and N. A. DeLuca.** 1994. The role of ICP4 repressor activity in temporal expression of the IE-3 and latency-associated transcript promoters during HSV-1 infection. Virology **202:**550–564.
59. **Rixon, F. J., M. E. Campbell, and J. B. Clements.** 1982. The immediate early mRNA that encodes the regulatory polypeptide Vmw 175 of herpes simplex virus type 1 is unspliced. EMBO J. **1:**1273–1277.
60. **Rock, D. L., A. B. Nesburn, H. Ghiasi, J. Ong, T. L. Lewis, J. R. Lokensgard, and S. L. Wechsler.** 1987. Detection of latency-related viral RNAs in trigeminal ganglia of rabbits infected with herpes simplex virus type 1. J. Virol. **61:**3820–3826.
61. **Saiki, R. K., D. H. Gelfand, S. Stoffel, S. J. Scharf, R. Higuchi, G. T. Horn, K. B. Mullis, and H. A. Erlich.** 1988. Primer-directed enzymatic amplification of DNA with a thermostable DNA polymerase. Science **239:**487–488.
62. **Sawtell, N. M., and R. L. Thompson.** 1992. Herpes simplex virus type 1 latency-associated transcription unit promotes anatomical site-dependent establishment and reactivation from latency. J. Virol. **66:**2157–2169.
63. **Sawtell, N. M., and R. L. Thompson.** 1992. Rapid in vivo reactivation of herpes simplex virus in latently infected murine ganglionic neurons after transient hyperthermia. J. Virol. **66:**2150–2156.
64. **Smith, R. L., L. I. Pizer, E. M. Johnson, Jr., and C. L. Wilcox.** 1992. Activation of second-messenger pathways reactivates latent herpes simplex virus in neuronal cultures. Virology **188:**311–318.
65. **Speck, P. G., and A. Simmons.** 1991. Divergent molecular pathways of productive and latent infection with a virulent strain of herpes simplex virus type 1. J. Virol. **65:**4001–4005.
66. **Spivack, J. G., and N. W. Fraser.** 1987. Detection of herpes simplex virus type 1 transcripts during latent infection in mice. J. Virol. **61:**3841–3847.
67. **Steiner, I., N. Mador, I. Reibstein, J. G. Spivack, and N. W. Fraser.** 1994. Herpes simplex virus type 1 gene expression and reactivation of latent infection in the central nervous system. Neuropathol. Appl. Neurobiol. **20:** 253–260.
68. **Steiner, I., J. G. Spivack, D. R. O'Boyle II, E. Laavi, and N. W. Fraser.** 1988. Latent herpes simplex virus type 1 transcription in human trigeminal ganglia. J. Virol. **62:**3493–3496.
69. **Stevens, J. G., and M. L. Cook.** 1971. Latent herpes simplex virus in spinal ganglia of mice. Science **173:**843–845.
70. **Stevens, J. G., E. K. Wagner, G. B. Devi-Rao, and M. L. Cook.** 1987. RNA complementary to a herpesvirus α gene mRNA is prominent in latently infected neurons. Science **235:**1056–1059.
71. **Suzuki, S., and J. R. Martin.** 1989. Herpes simplex virus type 2 transcripts in trigeminal ganglia during acute and latent infection in mice. J. Neurol. Sci. **93:**239–251.
72. **Tenser, R. B., W. A. Edris, and K. A. Hay.** 1993. Neuronal control of herpes simplex virus latency. Virology **195:**337–347.
73. **Tenser, R. B., W. A. Edris, K. A. Hay, and B. E. DeGalan.** 1991. Expression of herpes simplex virus type 2 latency-associated transcript in neurons and nonneurons. J. Virol. **65:**2745–2750.
74. **Tokunaga, K., H. Taniguchi, K. Yoda, M. Shimizu, and S. Sakiyama.** 1986. Nucleotide sequence of a full-length cDNA for mouse cytoskeleton β-actin mRNA. Nucleic Acids Res. **14:**2829.
75. **Tullo, A. B., C. Shimeld, W. A. Blyth, T. J. Hill, and D. L. Easty.** 1982. Spread of virus and distribution of latent infection following ocular herpes simplex in the non-immune and immune mouse. J. Gen. Virol. **63:**95–101.
76. **Vali-Nagy, T., S. Deshmane, A. Dillner, and N. W. Fraser.** 1991. Induction of cellular transcription factors in trigeminal ganglia of mice by corneal scarification, herpes simplex virus type 1 infection, and explantation of trigeminal ganglia. J. Virol. **65:**4142–4152.
77. **Wechsler, S. L., A. B. Nesburn, J. Zwaagstra, and H. Ghiasi.** 1989. Sequence of the latency-related gene of herpes simplex virus type 1. Virology **168:**168–172.
78. **Wilcox, C. L., R. L. Smith, C. R. Freed, and E. M. Johnson, Jr.** 1990. Nerve-growth factor-dependence of herpes simplex virus latency in peripheral sympathetic and sensory neurons *in vitro*. J. Neurosci. **10:**1268–1275.
79. **Wolffe, A. P.** 1991. Implications of DNA replication for eucaryotic gene expression. J. Cell Sci. **99:**201–206.